Optimizing the Optical Transparency at the Nanometer Level of Neodymium Oxide, Nd_2O_3, in Methanol Solutions

Hassane Aassaoudi , Clarisse Chiche-Lapierre , Ian S. Butler , Christopher J. Barrett *

Posted Date: 10 September 2025

doi: 10.20944/preprints202509.0848.v1

Keywords: neodymium oxide; nanoparticles; colloidal stabilization; optical transparency; quantum dots; nanoparticle synthesis; trioctylphosphine oxide capping; nanomaterials

 doi:10.20944/preprints202509.0848.v1

Article

Optimizing the Optical Transparency at the Nanometer Level of Neodymium Oxide, Nd_2O_3, in Methanol Solutions

Hassane Assaaoudi, Clarisse Chiche-Lapierre, Ian S. Butler and Christopher J. Barrett *

Department of Chemistry, McGill University, Montreal, QC, Canada

* Correspondence: christopher.barrett@mcgill.ca

Abstract

This study presents the synthesis and characterization of sub-5 nm neodymium oxide (Nd_2O_3) nanoparticles in methanol, utilizing trioctylphosphine oxide (TOPO) as a capping agent to achieve high chemical purity, phase control, and colloidal stability. By optimizing the NaOH/Nd molar ratio, monodisperse and ultrasmall nanoparticles with excellent optical transparency were produced, as confirmed by transmission electron microscopy, X-ray diffraction, UV-visible, infrared spectroscopy, and inductively coupled plasma analysis. The non-aqueous synthesis route effectively suppressed hydroxide formation, ensuring phase purity and enabling precise size tuning. The resulting Nd_2O_3 nanoparticle suspensions exhibited reversible aggregation and redispersibility, supporting their suitability for high-transparency detector media. These advances address critical requirements for neutrino detection experiments, such as those conducted at the Sudbury Neutrino Observatory (SNO), where minimal optical absorbance and long optical path lengths are essential for optimal performance. The findings inform future strategies for nanoparticle stabilization and integration, paving the way for scalable production of transparent nanomaterial solutions for next-generation neutrino detectors and other optoelectronic applications.

Keywords: neodymium oxide; nanoparticles; colloidal stabilization; optical transparency; quantum dots; nanoparticle synthesis; trioctylphosphine oxide capping; nanomaterials

1. Introduction

Investigations of quantum dots (QDs) in solution have led to a wide range of potential applications due to their unique, tunable optical and electronic properties, which are preserved and easily manipulated in the liquid phase. In optoelectronics, solution-processed QDs are used to fabricate devices such as light-emitting diodes (LEDs), photodetectors, and solar cells. The ability to process QDs from solution enables scalable, low-cost manufacturing and integration with flexible substrates, which is advantageous for next-generation electronic devices [1–4]. In the biomedical field, QDs in solution are highly valuable for bioimaging, biosensing, drug delivery, and diagnostics, due to their high photostability, tunable emission, and potential for biocompatibility (e.g., carbon and surface-modified QDs) [4–8]. QDs in solution are also widely used in environmental and analytical sensing. They serve as sensitive and selective fluorescent probes for detecting heavy metals, toxins, and other analytes in environmental and clinical samples. Their high surface area and modifiable surfaces allow for the development of sensors with high specificity and rapid response times. Additionally, QDs in solution are being explored for photocatalysis and environmental remediation, leveraging their strong light absorption and catalytic properties [4,7]. Another notable application is in radiation detection and scintillation. For example, lead halide perovskite QDs in liquid scintillators have shown promise for high-sensitivity X-ray and gamma-ray detection, with potential uses in medical imaging and radiation monitoring [9]. The solution-phase synthesis and processing of QDs

 doi:10.20944/preprints202509.0848.v1

also facilitate rapid screening of compositions, surface chemistries, and functional properties, accelerating research and development in all these fields [2,10].

Technological advancements in nanocomposite scintillator development have shown that QDs can be co-dispersed with other functional nanoparticles in a matrix, such as polymers or hydrogels, to enhance radiation detection capabilities. For example, scintillation compositions with QDs and optional neutron-capturing isotopes have been developed for improved neutron and gamma detection, demonstrating the feasibility of integrating multiple types of nanoparticles for synergistic effects [11,12].

Neutrino detection is inherently challenging due to the extremely weak interaction of neutrinos with matter, necessitating large detector volumes and underground placement to minimize interference from cosmic rays and background radiation. The Sudbury Neutrino Observatory (SNO) exemplifies this approach, employing 1,000 tons of ultrapure heavy water (D_2O) within a 12-meter acrylic vessel, surrounded by ultrapure ordinary water and an array of photodetectors sensitive to visible light (600–700 nm). This setup enables the detection of neutrino interactions, including the breaking apart of deuterium nuclei, which releases free neutrons that produce detectable gamma-ray bursts [13,14]. The ground-breaking discoveries made at SNO, culminating in the discovery of neutrino oscillations and the conclusion that neutrinos have mass, were recognized with the 2015 Nobel Prize in Physics, awarded jointly to Takaaki Kajita and Arthur B. McDonald (representing the SNO collaboration) [15]. The present work builds upon this foundation, aiming to advance neutrino detection technology through the development of novel nanomaterials for next-generation experiments.

QDs can significantly improve scintillation light yield and allow for spectral tunability, which are both advantageous for optimizing detector performance. Neodymium, particularly the isotope ^{150}Nd, is of special interest in neutrino physics for neutrinoless double-beta decay searches, so incorporating neodymium oxide nanoparticles (Nd_2O_3 NPs) could provide a high loading of the target isotope within the scintillator matrix. The solution-phase synthesis of QDs also allows for scalable fabrication and surface functionalization, which could facilitate the integration of both QDs and neodymium oxide nanoparticles into a single scintillating medium, offering modularity for tailoring detector properties to specific experimental needs [11,12]. Key technical challenges include ensuring compatibility between the two types of nanoparticles, maintaining optical transparency, and optimizing energy transfer mechanisms to maximize scintillation efficiency. Practical implementation would also need to address potential issues such as quenching effects, radiopurity, and long-term stability.

Previous successful collaborative work was reported between the Canadian SNO headed at Queen's University Physics by Professors Mark Chen and Arthur McDonald, and SNO-member McGill University Chemistry NP labs led by Prof. Christopher Barrett. In order to obtain sufficient Nd_2O_3 NPs for the SNO experiments, Dorris, Barrett, McDonald *et al*. [16] employed two synthetic polyelectrolytes, polystyrene sulfonate (PSS) and polyallylamine hydrochloride (PAH), as transparent stabilization coatings to the particles. These high molecular weight (~16,000 g/mol) polyelectrolytes act as strongly adsorbing surfactants to amplify surface charge and to disperse and stabilize the Nd2O3 NPs. The acid-base equilibria that take place on the surface of the particles have been investigated under different pH conditions in the absence and presence of the polyelectrolytes to optimize particle stabilization through enhancement of the effective repulsive surface charges. This approach has led to a 100-fold improvement in particle transparency in some parts of the visible region in neutral and acidic pH regimes, and to a 10-fold surface-charge amplification under basic pH conditions.

Advancements in nanoparticle stabilization techniques have broadened the potential of polyelectrolytes as stabilizing agents for Nd_2O_3 nanoparticles in large-scale particle physics experiments. For example, surface coatings with polydopamine (pDA) and bovine serum albumin (BSA) have been shown to improve biocompatibility and optical properties in lanthanide-based nanoparticles, which could be adapted for Nd_2O_3 systems [17]. Layer-by-layer (LBL) assembly

 doi:10.20944/preprints202509.0848.v1

techniques, involving alternating biopolymer layers, provide robust structural integrity and dispersion, making them suitable for achieving high optical transparency over long path lengths [18]. Permanently linked magnetic chains coated with polyelectrolyte layers, prepared using sol-gel or amidation methods, offer enhanced stability and functional properties that could be relevant for optical applications [19,20]. Additionally, aggregation-induced emission-active polyelectrolytes have demonstrated efficient photodynamic capabilities and could potentially be tailored for optical transparency in Nd_2O_3 nanoparticle systems [21]. Polyelectrolyte-wrapped nanometallic particles used in Surface Enhanced Raman Scattering (SERS) applications further showcase the versatility of polyelectrolytes in enhancing optical properties [22]. These advancements collectively highlight the evolving role of polyelectrolytes and related stabilization techniques in optimizing Nd_2O_3 nanoparticles for applications such as neutrino detection, where minimal optical absorbance and long optical path lengths are critical.

Recent advances in the synthesis and stabilization of rare-earth oxide nanoparticles, including Nd_2O_3, have significantly improved their colloidal stability and broadened their application potential. While traditional synthesis methods such as chemical vapor deposition [23,24], laser ablation [25,26], combustion [27–30], sol-gel [31], microemulsion [32], and hydrothermal techniques [33,34] remain foundational, the field has seen substantial progress through the adoption of advanced surface functionalization strategies. These include the use of polyelectrolyte coatings, layer-by-layer assembly, and biopolymer coatings, which have enabled the preparation of stable colloidal dispersions of lanthanide oxides—including Eu_2O_3, Tb_2O_3, and more recently, Nd_2O_3—in a variety of solvents [35,36]. These surface modification approaches enhance both electrostatic and steric stabilization, effectively preventing nanoparticle aggregation and precipitation. As a result, they lead to improved nanoparticle dispersion, optical transparency, and long-term stability, properties that are critical for applications in particle physics and optoelectronics. Notably, polyelectrolyte and biopolymer coatings not only stabilize the nanoparticles but can also tune their optical properties, making them more suitable for use in advanced devices and sensors. The successful extension of these stabilization methods to Nd_2O_3 nanoparticles marks a significant step forward, facilitating their use in scientific and technological applications where stable, transparent, and functional colloids are essential [37].

The primary goal of this paper is to synthesize neodymium oxide nanoparticles with diameters below 5 nm and to evaluate their stability in solution for potential use in high-transparency neutrino detection experiments, such as those conducted at the Sudbury Neutrino Observatory (SNO). This study systematically characterizes the morphologies, aggregation states, and optical transparencies of these sub-5 nm Nd_2O_3 nanoparticles in solutions without polyelectrolyte stabilizers, thereby elucidating their intrinsic colloidal behavior. The findings aim to inform future strategies for nanoparticle stabilization in neutrino detector media, where achieving minimal optical absorbance and supporting long optical path lengths are critical for optimal detector performance [38].

2. Materials and Methods

Nd_2O_3 nanoparticle synthesis.

All the reactions were performed at room temperature. 100 mL of a 5×10^{-3} M $Nd(NO_3)_3{\cdot}6H_2O$ solution in HPLC grade methanol was mixed for 10 min with 100 mL of a 5×10^{-3} M trioctylphosphine oxide (TOPO) solution in methanol. To this mixture was added dropwise 100 mL of a 5×10^{-2} M NaOH solution in methanol to precipitate the Nd_2O_3 NPs. The solution was stirred for a further 20 min. The resulting powders obtained after filtration were characterized by X-ray powder diffraction (XRD) and transmission electron microscopy (TEM), coupled with X-ray energy dispersive analysis (EDX), as well as by IR and UV–visible spectroscopic measurements. A Philips model PW1710, vertical goniometer, X-ray powder diffractometer with a Cu K_α radiation source was used for the powder diffraction measurements. The samples were scanned over a 10–60° range using a step size (2θ) of 0.02°. The morphology of the particles was investigated using a TEM Philips CM200 transmission electron microscope, operating at an acceleration voltage of 200 kV. The point-to-point and line

 doi:10.20944/preprints202509.0848.v1

resolutions of the microscope were 0.24 and 0.17 nm, respectively. The TEM was coupled to the EDS system. The TEM samples were preserved in methanol solution. The transparency of the NP suspensions was monitored by UV-visible spectroscopy on a Cary 500 UV-visible spectrophotometer using 1-cm quartz cuvettes. Absorbance measurements were recorded on 2.5 mL aliquots of the samples without any further dilution. Infrared spectra were obtained using a Perkin Elmer FTIR (Spectrum BX model) spectrometer with a Miracle single-bounce diamond ATR cell from PIKE Technologies. Spectra over the 4000–550 cm^{-1} range were obtained by the co-addition of 32 scans at a resolution of 4 cm^{-1}. ICP chemical analyses were performed on a Thermo Jarrell-Ash Trace Scan Axial Torch Sequential ICP system.

Use of GenAI.

The generative AI GEMA (Amass, accessed on 205/08/15 and 2025/09/04-05) was used for the purposes of text editing with the help of the AI's writer assistant function. GEMA's scientific assistant function was used to suggest relevant and up-to-date literature tailored to the research topics, to synthesize and summarize scientific papers, and to generate comprehensive reviews on selected subjects. The output was systematically reviewed and edited by the authors.

3. Results

In this section, we present results of the synthesis, chemical characterization, and colloidal behaviour of sub-5 nm neodymium oxide (Nd_2O_3) nanoparticles in methanol, with a focus on their stability and optical transparency for neutrino detection applications. Specifically, we employed electron diffraction, electron microscopy, and UV-Visible spectrophotometry to characterize the particles, and assess the effects of synthesis variables on the transparency. These findings provide insight into how synthesis conditions influence nanoparticle morphology, composition, and solution stability, which are critical parameters for their use in the Sudbury Neutrino Observatory.

Nd_2O_3 NPs were synthetised by mixing equimolar 5 x 10^{-3} M solutions of $Nd(NO_3)_3$ and trioctylphosphine oxide (TOPO) in methanol, followed by drop-wise addition of NaOH in methanol. The transmission electron microscopy (TEM) analysis, shown in Figure 1, demonstrates that the synthesized Nd_2O_3 nanoparticles exhibit a narrow size distribution between 2 and 5 nm, which is significantly smaller than many other oxide nanoparticles and beneficial for high surface area applications [39,40].

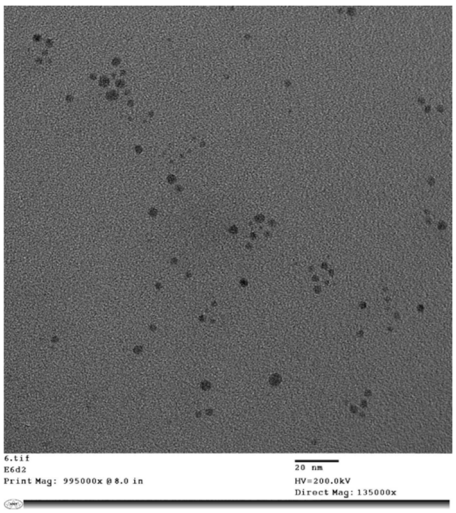

Figure 1. TEM image of Nd_2O_3 nanoparticles.

Energy-dispersive X-ray (EDX) spectroscopy (Figure 2) confirmed the presence of neodymium, oxygen, and carbon, the latter likely arising from the capping agent, as similarly observed in other nanomaterial systems [41,42]. The precipitation of Nd_2O_3 NPs was conducted in a non-aqueous medium to suppress the formation of $Nd(OH)_3$, ensuring phase purity [43]. To prevent particle

 doi:10.20944/preprints202509.0848.v1

agglomeration, TOPO was employed as a surface capping agent, which not only stabilizes the nanoparticles but also passivates surface states, reducing non-radiative recombination via dangling bond states and enhancing optical properties [44–47].

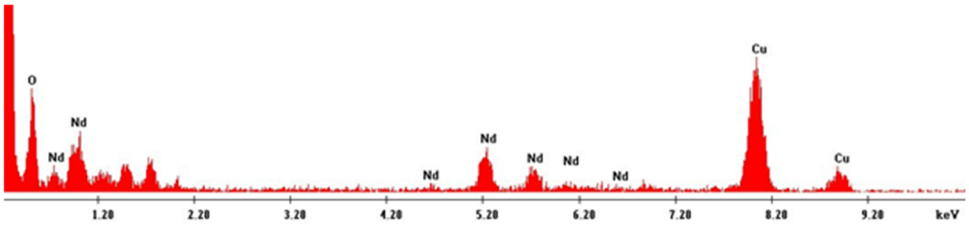

Figure 2. Electron diffraction (ED) of Nd_2O_3 nanoparticles.

Inductively coupled plasma (ICP) analysis confirmed that the synthesized Nd_2O_3 NPs achieved a high chemical purity of 97.5% when a NaOH/Nd molar ratio of 7.8 was employed. Reducing the volume of 0.05 M sodium hydroxide in methanol from 100 mL to 26 mL, thereby lowering the NaOH/Nd ratio to 2.6, resulted in a decreased Nd_2O_3 content of 89.4%, highlighting the critical role of base concentration in ensuring complete oxide formation during synthesis.

Infrared (IR) spectroscopy of the dried nanoparticles revealed spectra identical to commercial Nd_2O_3, with no additional vibrational bands between 4000–400 cm^{-1}, confirming phase purity and the absence of significant organic or hydroxide impurities. In contrast, attempts to synthesize Nd_2O_3 in aqueous solution yielded only the hydroxide phase, emphasizing the necessity of the methanol/NaOH system for direct oxide formation. Transmission electron microscopy (TEM) analysis demonstrated that the NaOH/Nd ratio effectively controlled particle size: a ratio of 2.6 produced nanoparticles averaging 2–3 nm, while a ratio of 7.8 resulted in larger particles of 4–5 nm, consistent with the established influence of base concentration on nanoparticle growth dynamics [48].

UV-visible spectroscopy showed a progressive decrease in absorbance intensity over 1, 2, and 7 days, indicative of reversible aggregation or sedimentation in suspension (Figure 3); notably, ultrasonic stirring restored the original absorbance, confirming the colloidal stability and redispersibility of the nanoparticles. Collectively, these findings demonstrate that the NaOH/Nd molar ratio in methanol not only governs the chemical purity and phase of Nd_2O_3 nanoparticles but also enables precise control over particle size, while the nanoparticles exhibit reversible aggregation behavior in suspension.

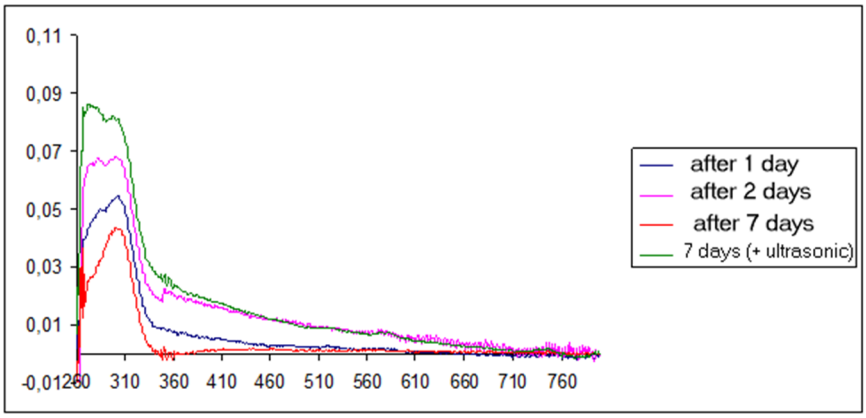

Figure 3. UV-visible spectra of a set of measurements taken after 1, 2 and 7 days from the same sample at the top of the reaction vessel. Ultrasonic stirring of the sample greatly in-creases the intensity (green curve).

The evolution of optical properties during the synthesis of Nd_2O_3 NPs was investigated using UV-visible spectroscopy, with particular attention to the effects of pH, temperature, and precursor

 doi:10.20944/preprints202509.0848.v1

concentration. Initially, mixing equimolar 5 x 10^{-3} M solutions of $Nd(NO_3)_3$ and TOPO in methanol produced a transparent solution with no visible precipitation, exhibiting three distinct absorption peaks at 747, 587, and 279 nm (Figure 4a). To this mixture, a solution of NaOH in methanol was added dropwise, with no immediate affect on the absorption profile, indicating that neodymium remained soluble and no nanoparticle formation had occurred. After the addition of 30 drops of NaOH, the mixture remained transparent but a strong new absorption band at 271 nm appeared, overlapping the original weak bands at 587 and 747 nm (Figure 5b). This spectral change marked the onset of Nd_2O_3 NP formation and corresponded to the system's maximum neodymium solubility. The persistence of transparency at this stage suggests the formation of a colloidal dispersion of ultrasmall nanoparticles or clusters, consistent with early nucleation phenomena observed in other nanoparticle systems [49].

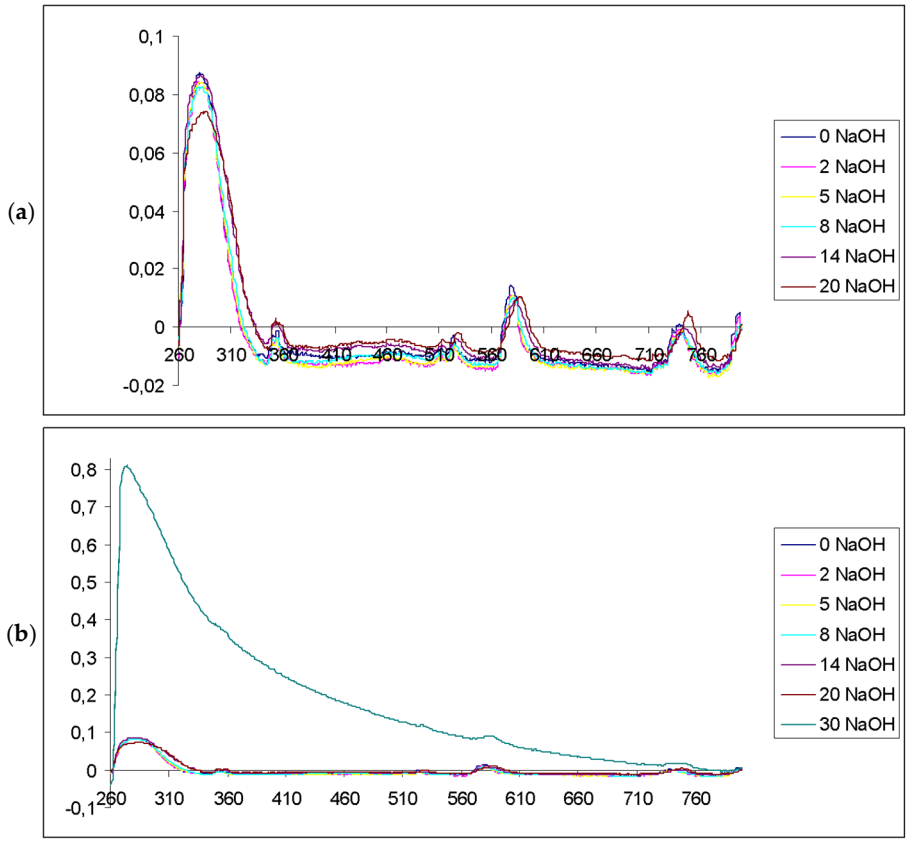

Figure 4. UV-visible spectra of the reaction mixture, $Nd(NO_3)_3$ and TOPO, before and after addition of NaOH (**a**) UV-visible spectra of the reaction mixture, $Nd(NO_3)_3$ and TOPO, before the pH threshold of precipitation (between 21 and 30 drops); (**b**) UV-visible spectra of the reaction mixture, $Nd(NO_3)_3$ and TOPO, including measurement after the pH threshold of precipitation (30 drops).

 doi:10.20944/preprints202509.0848.v1

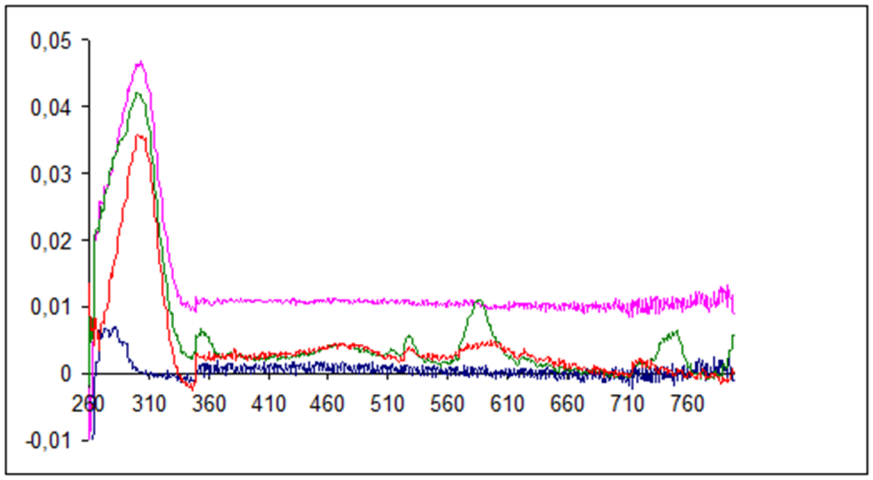

Figure 5. UV-Visible spectra of samples from different experiments.

4. Discussion

The maximum solubility of neodymium was found to be dependent on both pH and the initial concentrations of $Nd(NO_3)_3$ and TOPO. Increasing the pH by further NaOH addition promoted spontaneous precipitation of Nd_2O_3 NPs, in line with the reduced solubility of metal oxides at higher pH [49]. UV-visible spectra of filtrates from different experiments were similar (Figure 5), indicating comparable neodymium concentrations across samples. Some spectra retained the pre-precipitation bands, while others showed only the 271 nm band; over time, all bands except the 271 nm band disappeared, reflecting dynamic changes in the colloidal state and the progressive conversion of soluble neodymium species to nanoparticulate Nd_2O_3.

Concentration of the filtrates by slow methanol evaporation was feasible, supporting the colloidal stability of the system prior to precipitation. Both pH and temperature influenced the maximum achievable neodymium concentration, with higher pH and temperature accelerating the transition from soluble species to precipitated nanoparticles. These findings are consistent with established principles regarding the impact of pH and temperature on nanoparticle nucleation, growth, and optical properties [49,50]. Overall, UV-visible spectroscopic monitoring revealed distinct stages in the evolution of optical properties, closely linked to changes in neodymium speciation and colloidal state, underscoring the dynamic interplay between pH, temperature, and precursor concentration in governing Nd_2O_3 NP synthesis.

Upon investigating the influence of temperature and NaOH/Nd molar ratio on the optical properties of Nd_2O_3 NPs, UV-visible spectroscopy of the supernatant after overnight reflux revealed a distinct pink coloration (Figure 6a), indicative of neodymium-containing species or nanoparticle formation [51]. Systematic variation of the NaOH/Nd reactant ratio from 1:2.6 to 1:5.3 and 1:7.8 demonstrated that the maximum optical absorption (pink spectrum, Figure 6b) occurred at a 1:2.6 ratio, establishing this condition as optimal for Nd_2O_3 NP synthesis. At a 1:5.3 ratio, the optical absorption decreased (red spectrum), while a further increase to 1:7.8 resulted in a slight absorption increase (green spectrum). These results highlight the critical role of the NaOH/Nd ratio and pH in modulating nanoparticle formation, solubility, and optical response, with the observed spectral changes reflecting the transition from soluble neodymium species to nanoparticulate Nd_2O_3. Such tunability of optical properties with synthesis parameters is consistent with trends observed in other nanomaterial systems, where composition and reaction conditions directly impact absorption characteristics [49–53].

 doi:10.20944/preprints202509.0848.v1

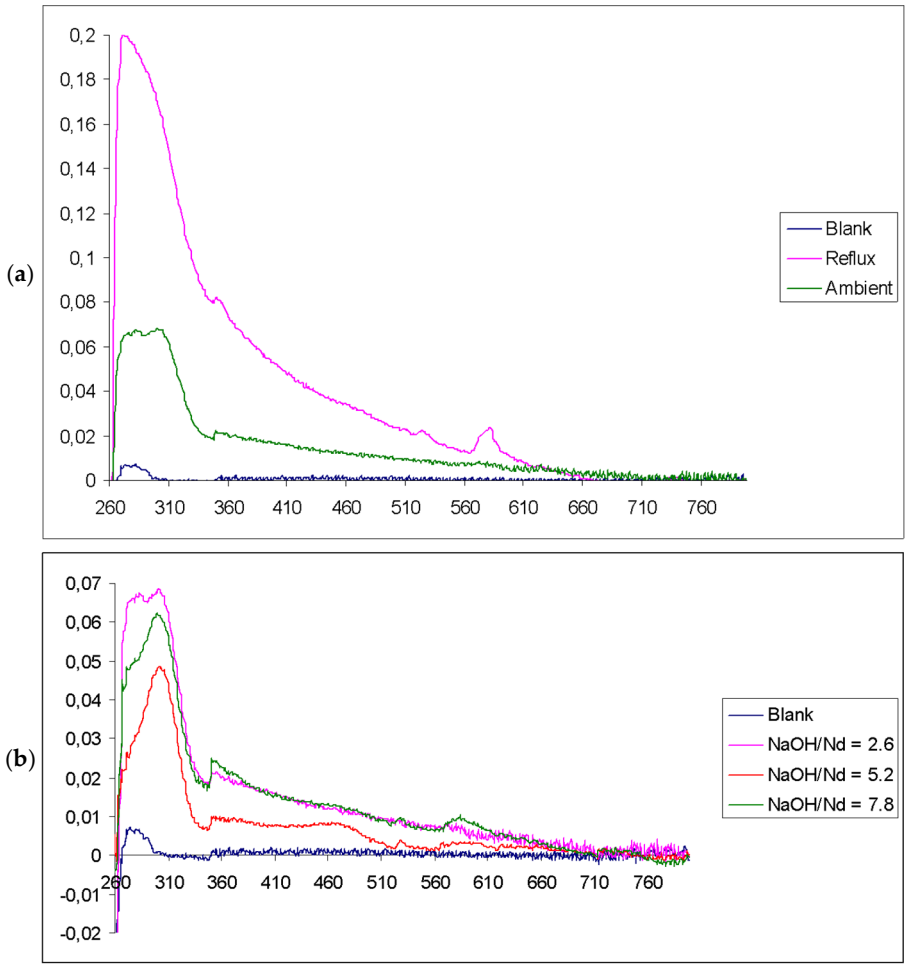

Figure 6. UV-Visible spectra Nd_2O_3 nanoparticles solution: (**a**) Spectra of clear solution of nanoparticles obtained at ambient temperature (green) and the same solution treated by reflux heating (red); (**b**) Spectra of transparent solution of nanoparticles obtained at pH corresponding to ratio Nd/NaOH = 2.6 (pink), 5.2 (red), 7.8 (green).

5. Conclusions

The controlled synthesis of Nd_2O_3 nanoparticles (NPs) in a methanol/NaOH system with TOPO as a capping agent enables the production of ultrasmall, monodisperse, and phase-pure nanoparticles with tunable size and high chemical purity. Nd_2O_3 NPs with a sub-5 nm size were successfully synthesized with high phase purity and excellent colloidal stability in methanol, achieved with an optimal NaOH/Nd molar ratio of 2.6. The NaOH/Nd molar ratio is a key parameter that governs both the chemical composition and particle size, while the non-aqueous medium is essential for suppressing hydroxide formation and ensuring phase purity. This approach yields optically transparent methanol solutions of Nd_2O_3 NPs, which is a critical requirement for their application in neutrino detection, where minimizing light scattering and maximizing detector sensitivity are essential. The comprehensive characterization of particle size distribution, phase purity, chemical composition, and optical properties confirms the intrinsic stability and suitability of these nanoparticles for use in high-transparency detector media. Importantly, the feasibility of producing large volumes of these transparent solutions opens a promising pathway for their deployment in large-scale neutrino detection experiments at the Sudbury Neutrino Observatory (SNO), directly supporting next-generation neutrino detectors that require stable, transparent nanoparticle solutions [54].

 doi:10.20944/preprints202509.0848.v1

Author Contributions: Conceptualization, I.B., C.B.; methodology, I.B., C.B.; investigation, H.A., C.C-L.; resources, C.B., I.B.; writing—original draft preparation, H.A., C.C-L.; writing—review and editing, C.C-L., C.B.; supervision, I.B., C.B.; project administration, C.B. I.B.; funding acquisition, C.B., I.B; All authors have read and agreed to the published version of the manuscript.

Funding: This research was supported by NSERC Canada discovery grants to I.S.B and C.J.B of McGill University, and H.A. acknowledges support of Postdoctoral funding directly from SNO Canada, and Director Arthur McDonald of Queen's University.

Acknowledgments: The authors are grateful to SNO Director Prof. Arthur McDonald of Queen's U. Physics for discussions that enabled this project, and for travel between Queen's and McGill by both Barrett and McDonald which assisted oversight and direction of the project. During the preparation of this manuscript, the authors used GEMA (Amass, accessed on 205/08/15 and 2025/09/04-05) for the purposes of text editing with the help of the AI's writer assistant function, to enhance the clarity, coherence, and style of the scientific texts. GEMA's scientific assistant function was used to suggest relevant and up-to-date literature tailored to the research topics; to synthesize and summarize scientific papers for improved understanding and integration of findings; and to generate comprehensive, state-of-the-art reviews on selected subjects. The authors have reviewed and edited the output and take full responsibility for the content of this publication.

Conflicts of Interest: The authors declare no conflicts of interest.

Abbreviations

The following abbreviations are used in this manuscript:

Nd_2O_3	Neodymium oxide
NP	Nanoparticles
TOPO	Trioctylphosphine oxide
QDs	Quantum dots
LEDs	Light-emitting diodes
SNO	Sudbury Neutrino Observatory
PSS	Polystyrene sulfonate
PAH	Polyallylamine hydrochloride
pDA	Polydopamine
BSA	Bovine serum albumin
LBL	Layer-by-layer
SERS	Surface Enhanced Raman Scattering
HPLC	High-performance liquid chromatography
XRD	X-ray powder diffraction
TEM	Transmission electron microscopy
EDX	X-ray energy dispersive analysis
ICP	Inductively coupled plasma
IR	Infrared

References

1. Saleem, M.I.; Yang, S.; Sulaman, M.; Hu, J.; Chandrasekar, P.V.; Shi, Y.; Zhi, R.; Batool, A.; Zou, B. All-Solution-Processed UV-IR Broadband Trilayer Photodetectors with $CsPbBr_3$ Colloidal Nanocrystals as Carriers-Extracting Layer. *Nanotechnology* **2020**, *31*, 165502.
2. Sevim Ünlütürk, S.; Taşcıoğlu, D.; Özçelik, S. Colloidal Quantum Dots as Solution-Based Nanomaterials for Infrared Technologies. *Nanotechnology* **2025**, *36*, 082001.
3. Huang, C.-Y.; Li, H.; Wu, Y.; Lin, C.-H.; Guan, X.; Hu, L.; Kim, J.; Zhu, X.; Zeng, H.; Wu, T. Inorganic Halide Perovskite Quantum Dots: A Versatile Nanomaterial Platform for Electronic Applications. *Nano-Micro Lett.* **2023**, *15*, 16.
4. Mondal, J.; Lamba, R.; Yukta, Y.; Yadav, R.; Kumar, R.; Pani, B.; Singh, B. Advancements in Semiconductor Quantum Dots: Expanding Frontiers in Optoelectronics, Analytical Sensing, Biomedicine, and Catalysis. *J. Mater. Chem. C* **2024**, *12*, 10330–10389.

 doi:10.20944/preprints202509.0848.v1

5. Phafat, B.; Bhattacharya, S. Quantum Dots as Theranostic Agents: Recent Advancements, SurfaceModifications, and Future Applications. *Mini-Rev. Med. Chem.* **2023**, *23*, 1257–1272.
6. Gour, A.; Ramteke, S.; Jain, N.K. Pharmaceutical Applications of Quantum Dots. *AAPS PharmSciTech* **2021**, *22*, 233.
7. Kong, J.; Wei, Y.; Zhou, F.; Shi, L.; Zhao, S.; Wan, M.; Zhang, X. Carbon Quantum Dots: Properties, Preparation, and Applications. *Molecules* **2024**, *29*, 2002.
8. Singh, S.; Raina, D.; Rishipathak, D.; Babu, K.R.; Khurana, R.; Gupta, Y.; Garg, K.; Rehan, F.; Gupta, S.M. Quantum Dots in the Biomedical World: A Smart Advanced Nanocarrier for Multiple Venues Application. *Arch. Pharm. (Weinheim)* **2022**, *355*, 2200299.
9. Xu, Q.; Huang, J.; Liu, J.; Wang, J.; Zhou, S.; Wang, X.; Nie, J.; Guo, Y.; Ouyang, X. Lead Halide Perovskite Quantum Dots Based Liquid Scintillator for X-Ray Detection. *Nanotechnology* **2021**, *32*, 205201.
10. Efros, A.L.; Brus, L.E. Nanocrystal Quantum Dots: From Discovery to Modern Development. *ACS Nano* **2021**, *15*, 6192–6210.
11. Delage, M.-È.; Lecavalier, M.-È.; Larivière, D.; Allen, C.N.; Beaulieu, L. Preliminary Investigation of a Luminescent Colloidal Quantum Dots-Based Liquid Scintillator. *J. Phys. Conf. Ser.* **2017**, *847*, 012043.
12. Riddle Catherine L , Scates Dawn M , Fronk Ryan G , Demmer Rick L , Ghosh Priyarshini Scintillation Compositions And Related Hydrogels For Neutron And Gamma Radiation Detection, And Related Detection Systems And Methods 2025.
13. Shimizu, I.; Chen, M. Double Beta Decay Experiments With Loaded Liquid Scintillator. *Front. Phys.* **2019**, *7*, 33.
14. Chen, M.C. The SNO+ Experiment *JINST* 2021, 16, P08059.
15. The Nobel Prize in Physics 2015. *NobelPrize.org* 2025.
16. Dorris, A.; Sicard, C.; Chen, M.C.; McDonald, A.B.; Barrett, C.J. Stabilization of Neodymium Oxide Nanoparticles via Soft Adsorption of Charged Polymers. *ACS Appl. Mater. Interfaces* **2011**, *3*, 3357–3365.
17. Deng, K.; Liu, D.; Wang, Z.; Zhou, Z.; Chen, Q.; Luo, J.; Zhang, Y.; Hou, Z.; Lin, J. Surface-Functionalized NdVO4:Gd3+ Nanoplates as Active Agents for Near-Infrared-Light-Triggered and Multimodal-Imaging-Guided Photothermal Therapy. *Pharmaceutics* **2022**, *14*, 1217.
18. Matsunaga, T.O.; Alcaraz, P.; Witte, R.S. Nanodroplet With Layer-By-Layer Assembly. US Patent App. 17/778,733, 2022.
19. Singh, H.; Hatton, T.A. Permanently Linked, Rigid, Magnetic Chains. US Patent 7,332,101, 2008.
20. Singh, H; Hatton, T.A. Permanently Linked Magnetic Chains. US Patent 8,827,612, 2006.
21. Su, X.; Liu, R.; Li, Y.; Han, T.; Zhang, Z.; Niu, N.; Kang, M.; Fu, S.; Wang, D.; Wang, D.; et al. Aggregation-Induced Emission-Active Poly(Phenyleneethynylene)s for Fluorescence and Raman Dual-Modal Imaging and Drug-Resistant Bacteria Killing. *Adv. Healthc. Mater.* **2021**, *10*, 2101167.
22. Sivapalan, S.T.; DeVetter, B.M.; Yang, T.K.; Schulmerich, M.V.; Bhargava, R.; Murphy, C.J. Surface-Enhanced Raman Spectroscopy of Polyelectrolyte-Wrapped Gold Nanoparticles in Colloidal Suspension. *J. Phys. Chem. C* **2013**, *117*, 10677–10682.
23. Konrad, A.; Fries, T.; Gahn, A.; Kummer, F.; Herr, U.; Tidecks, R.; Samwer, K. Chemical Vapor Synthesis and Luminescence Properties of Nanocrystalline Cubic Y2O3:Eu. *J. Appl. Phys.* **1999**, *86*, 3129–3133.
24. Tomellini, M.; Gozzi, D.; Latini, A. Nanodusting of RENi5 Intermetallic Grains through Nucleation and Growth of Carbon Nanotubes (RE : Rare-Earth). *J. Phys. Chem. C* **2007**, *111*, 3266–3274.
25. Ledoux, G.; Amans, D.; Dujardin, C.; Masenelli-Varlot, K. Facile and Rapid Synthesis of Highly Luminescent Nanoparticles via Pulsed Laser Ablation in Liquid. *Nanotechnology* **2009**, *20*, 445605.
26. Eilers, H.; Tissue, B.M. Laser Spectroscopy of Nanocrystalline Eu2O3 and Eu3+:Y2O3. *Chem. Phys. Lett.* **1996**, *251*, 74–78.
27. Hao, J.; Studenikin, S.A.; Cocivera, M. Blue, Green and Red Cathodoluminescence of Y2O3 Phosphor Films Prepared by Spray Pyrolysis. *J. Lumin.* **2001**, *93*, 313–319.
28. Kang, Y.C.; Roh, H.S.; Park, S.B. Preparation of Y2O3:Eu Phosphor Particles of Filled Morphology at High Precursor Concentrations by Spray Pyrolysis. *Adv. Mater.* **2000**, *12*, 451–453.
29. Kang, Y.C.; Roh, H.S.; Park, S.B.; Park, H.D. [No Title Found]. *J. Mater. Sci. Lett.* **2002**, *21*, 1027–1029.

 doi:10.20944/preprints202509.0848.v1

30. Dosev, D.; Guo, B.; Kennedy, I.M. Photoluminescence of as an Indication of Crystal Structure and Particle Size in Nanoparticles Synthesized by Flame Spray Pyrolysis. *J. Aerosol Sci.* **2006**, *37*, 402–412.
31. Guo, H.; Dong, N.; Yin, M.; Zhang, W.; Lou, L.; Xia, S. Visible Upconversion in Rare Earth Ion-Doped Gd2O3 Nanocrystals. *J. Phys. Chem. B* **2004**, *108*, 19205–19209.
32. Zhang, J.; Ju, X.; Wu, Z.Y.; Liu, T.; Hu, T.D.; Xie, Y.N.; Zhang, Z.L. Structural Characteristics of Cerium Oxide Nanocrystals Prepared by the Microemulsion Method. *Chem. Mater.* **2001**, *13*, 4192–4197.
33. Assaaoudi, H.; Fang, Z.; Barralet, J.E.; Wright, A.J.; Butler, I.S.; Kozinski, J.A. Synthesis, Characterization and Properties of Erbium-Based Nanofibres and Nanorods. *Nanotechnology* **2007**, *18*, 445606.
34. Assaaoudi, H.; Fang, Z.; Butler, I.S.; Kozinski, J.A. Synthesis of Erbium Hydroxide Microflowers and Nanostructures in Subcritical Water. *Nanotechnology* **2008**, *19*, 185606.
35. Wakefield, G.; Keron, H.A.; Dobson, P.J.; Hutchison, J.L. Synthesis and Properties of Sub-50-Nm Europium Oxide Nanoparticles. *J. Colloid Interface Sci.* **1999**, *215*, 179–182.
36. Wakefield, G.; Keron, H.A.; Dobson, P.J.; Hutchison, J.L. Structural and Optical Properties of Terbium Oxide Nanoparticles. *J. Phys. Chem. Solids* **1999**, *60*, 503–508.
37. Sakka, Y. Particle Processing Technology. *Sci. Technol. Adv. Mater.* **2014**, *15*, 010201.
38. Rasp, J.; Eichholz, R.; Glass For Radiation And/or Particle Detectors US Patent App. 18/475,925, 2024.
39. Fischer, D.K.; Rodrigues De Fraga, K.; Scheeren, C.W. Ionic Liquid/TiO_2 Nanoparticles Doped with Non-Expensive Metals: New Active Catalyst for Phenol Photodegradation. *RSC Adv.* **2022**, *12*, 2473–2484
40. Alaghmandfard, A.; Madaah Hosseini, H.R. A Facile, Two-Step Synthesis and Characterization of Fe3O4–LCysteine–Graphene Quantum Dots as a Multifunctional Nanocomposite. *Appl. Nanosci.* **2021**, *11*, 849–860.
41. Sidhu, A.K.; Verma, N.; Kaushal, P. Role of Biogenic Capping Agents in the Synthesis of Metallic Nanoparticles and Evaluation of Their Therapeutic Potential. *Front. Nanotechnol.* **2022**, *3*, 801620.
42. Javed, R.; Zia, M.; Naz, S.; Aisida, S.O.; Ain, N.U.; Ao, Q. Role of Capping Agents in the Application of Nanoparticles in Biomedicine and Environmental Remediation: Recent Trends and Future Prospects. *J. Nanobiotechnology* **2020**, *18*, 172.
43. Koch, U.; Fojtik, A.; Weller, H.; Henglein, A. Photochemistry of Semiconductor Colloids. Preparation of Extremely Small ZnO Particles, Fluorescence Phenomena and Size Quantization Effects. *Chem. Phys. Lett.* **1985**, *122*, 507–510.
44. Tian, Y.; Fendler, J.H. Langmuir−Blodgett Film Formation from Fluorescence-Activated, Surfactant-Capped, Size-Selected CdS Nanoparticles Spread on Water Surfaces. *Chem. Mater.* **1996**, *8*, 969–974.
45. Khrebtov, A.I.; Danilov, V.V.; Kulagina, A.S.; Reznik, R.R.; Skurlov, I.D.; Litvin, A.P.; Safin, F.M.; Gridchin, V.O.; Shevchuk, D.S.; Shmakov, S.V.; et al. Influence of TOPO and TOPO-CdSe/ZnS Quantum Dots on Luminescence Photodynamics of InP/InAsP/InPHeterostructure Nanowires. *Nanomaterials* **2021**, *11*, 640.
46. Murray, C.B.; Norris, D.J.; Bawendi, M.G. Synthesis and Characterization of Nearly Monodisperse CdE (E = Sulfur, Selenium, Tellurium) Semiconductor Nanocrystallites. *J. Am. Chem. Soc.* **1993**, *115*, 8706–8715.
47. Ma, J. Preparation and Characterization of ZrO2 Nanoparticles Capped by Trioctylphosphine Oxide (TOPO). *J. Wuhan Univ. Technol.-Mater Sci Ed* **2011**, *26*, 611–614.
48. He, X.; Li, W.; Fang, B.; Zhang, S.; Lu, X.; Ding, J. Optimization Hydrothermal Synthesis Conditions for Nano-sized ($Na_{0.5}$ $Bi_{0.495}$ $Nd_{0.005}$)TiO_3 Particles by an Orthogonal Experiment and Their Luminescence Performance. *Luminescence* **2021**, *36*, 928–936.
49. Tamang, M.; Sapkota, K.P.; Shrestha, S. Effect of pH, Amount of Metal Precursor, and Reduction Time on The Optical Properties and Size of Zinc Oxide Nanoparticles Synthesized Using Aqueous Extract of Rhizomes of Acorus Calamus. *J. Nepal Chem. Soc.* **2024**, *44*, 16–30.
50. Anuar, M.F.; Fen, Y.W.; Zaid, M.H.M.; Omar, N.A.S.; Khaidir, R.E.M. Sintering Temperature Effect on Structural and Optical Properties of Heat Treated Coconut Husk Ash Derived SiO2 Mixed with ZnO Nanoparticles. *Materials* **2020**, *13*, 2555.
51. Jayarambabu, N.; Velupla, S.; Akshaykranth, A.; Anitha, N.; Rao, T.V. Bambusa Arundinacea Leaves Extract-Derived Ag NPs: Evaluation of the Photocatalytic, Antioxidant, Antibacterial, and Anticancer Activities. *Appl. Phys. A* **2023**, *129*, 13.

 doi:10.20944/preprints202509.0848.v1

52. Khatun, R.; Mamun, M.S.A.; Islam, S.; Khatun, N.; Hakim, M.; Hossain, M.S.; Dhar, P.K.; Barai, H.R. Phytochemical-Assisted Synthesis of Fe3O4 Nanoparticles and Evaluation of Their Catalytic Activity. *Micromachines* **2022**, *13*, 2077.
53. Chao, L.; Sun, C.; Dou, J.; Li, J.; Liu, J.; Ma, Y.; Xiao, L. Tunable Transparency and NIR-Shielding Properties of Nanocrystalline Sodium Tungsten Bronzes. *Nanomaterials* **2021**, *11*, 731.
54. Rasp, J.; Eichholz, R. Glass For Radiation And/Or Particle Detectors. US Patent App. 18/475,925, 2024.